

Article

Comparison between Self-Raman Nd:YVO₄ Lasers and NdYVO₄/KGW Raman Lasers at Lime and Orange Wavelengths

Chi-Chun Lee ^{1,2}, Chien-Yen Huang ^{1,2}, Hao-Yun Huang ^{1,2}, Chao-Ming Chen ^{1,2} and Chia-Han Tsou ^{1,2,*}

¹ Department of Electrophysics, National Yang Ming Chiao Tung University, Hsinchu 30010, Taiwan; a8507231996@gmail.com (C.-C.L.); so3355589@gmail.com (C.-Y.H.); a0970582090@gmail.com (H.-Y.H.); wade0106@gmail.com (C.-M.C.)

² NYCU-LIGHTMED Laser System Research Center, National Yang Ming Chiao Tung University, Hsinchu 30010, Taiwan

* Correspondence: ck315agan@hotmail.com

Abstract: The comparison of output powers between self-Raman Nd:YVO₄ lasers and Nd:YVO₄/KGW Raman lasers operating at lime and orange wavelengths is presented. We exploit the LBO crystal with cutting angle $\theta = 90^\circ$ and $\varphi = 8^\circ$ for the lime wavelengths, and then we change the angle to $\theta = 90^\circ$ and $\varphi = 3.9^\circ$ for the orange wavelengths. In self-Raman Nd:YVO₄ lasers, experimental results reveal that thermal loading can impact on the output performances, especially at the high pump power. However, by using a KGW crystal as Raman medium can remarkably share the thermal loading from gain medium. Besides, the designed coating for high reflectivity at the Stokes field on the surface of KGW also improved the beam quality and reduced the lasing threshold. For self-Raman Nd:YVO₄ lasers, we have achieved the output powers of 6.54 W and 5.12 W at 559 nm and 588 nm, respectively. For Nd:YVO₄/KGW Raman lasers, the output powers at 559 nm and 589 nm have been increased to 9.1 W and 7.54 W, respectively. All lasers operate at a quasi-CW regime with the repetition rate 50 Hz and the duty cycle 50%.

Keywords: Raman laser; visible light; solid-state laser

check for
updates

Citation: Lee, C.-C.; Huang, C.-Y.; Huang, H.-Y.; Chen, C.-M.; Tsou, C.-H. Comparison between Self-Raman Nd:YVO₄ Lasers and NdYVO₄/KGW Raman Lasers at Lime and Orange Wavelengths. *Appl. Sci.* **2021**, *11*, 11068. <https://doi.org/10.3390/app112211068>

Academic Editor: John Xiupu Zhang

Received: 20 October 2021

Accepted: 18 November 2021

Published: 22 November 2021

Publisher's Note: MDPI stays neutral with regard to jurisdictional claims in published maps and institutional affiliations.



Copyright: © 2021 by the authors. Licensee MDPI, Basel, Switzerland. This article is an open access article distributed under the terms and conditions of the Creative Commons Attribution (CC BY) license (<https://creativecommons.org/licenses/by/4.0/>).

1. Introduction

The lasers operating in the visible range of 500–600 nm have been paid attention to in recent decades because they have greatly been growing requirements of cancer phototherapy [1], retinal laser therapy [2], laser sodium guide stars [3], and projection displays [4]. Stimulated Raman scattering (SRS) process combining with intracavity second harmonic generation (SHG) and sum frequency generation (SFG) has been identified as an efficient and convenient method for generating the light source at 500–600 nm in solid-state lasers [5–18]. Since the Stokes field is quite sensitive to the losses of cavity, enhancing the reflectivity of resonator and reducing the losses of Stokes field as much as possible are important techniques to improve the output characteristics significantly [19,20].

Self-Raman laser implies that the fundamental wave and Stokes fields are generated in the one crystal, which offers several benefits with regard to compactness and minimizing the losses of cavity [21,22]. However, for the self-Raman laser, the strong thermal loading in the gain medium usually leads to the thermal fracture and confines the output power. Therefore, employing another crystal as a Raman medium is a practical way to reduce the risk of thermal fracture. Moreover, it also provides the wavelength versatility by using the different Raman shifts of Raman crystals. Potassium gadolinium tungstate (KGW) has been recognized as an outstanding Raman medium because of its high damage threshold, high Raman gain, two strong Raman shifts, and excellent thermal properties [23–25]. As a result, using KGW crystals as Raman media is a practical way to realize the high-powered and reliable Raman laser at 500–600 nm.

In this work, we demonstrate the comparison between self-Raman Nd:YVO₄ lasers and Nd:YVO₄/KGW Raman lasers at lime and orange wavelengths. The first Stokes fields

at 1176 nm and near 1178 nm are generated by a self-Raman Nd:YVO₄ crystal and a N_p-cut KGW crystal with the shift of 890 cm⁻¹ and 901 cm⁻¹, respectively. Based on the 1176 nm Stokes fields and the 1064 nm fundamental wave, we can achieve the lime at 559 nm and the orange at 588 nm in the self-Raman Nd:YVO₄ lasers with intracavity SFG and SHG. Similarly, the 559 nm and 589 nm can be obtained in the Nd:YVO₄/KGW Raman lasers. In addition, we separate the resonator of the Stokes field from that of fundamental wave by depositing a specific coating on the surface of KGW crystal toward the Nd:YVO₄ crystal. Due to employ the KGW crystal to share the thermal loading from the SRS process and the usage of the designed coating, we can find that a maximum output power and an optical conversion efficiency are superior to the self-Raman Nd:YVO₄ lasers at the high pump power. With the incident pump power of 40 W, the output powers including the lime and orange wavelengths can increase from 6.54 W to 9.1 W and from 5.12 W to 7.54 W, respectively.

2. Experimental Setup

Figure 1 demonstrates two types of experimental setups for generating the 559 nm and 589 nm beams. One type shown in Figure 1a illustrated that we used a size of 3 × 3 × 20 mm³ a-cut 0.3-at.% Nd:YVO₄ crystal as the gain medium and the Raman active medium at the same time. The facet of the Nd:YVO₄ crystal toward the pump was coated high reflectance (R > 99.9%) at 1030–1200 nm and high transmission at 808 nm (T > 95%). The second type was that an a-cut 0.35-at.% Nd:YVO₄ crystal with the dimension of 3 × 3 × 10 mm³ was utilized to generate the fundamental wave. Moreover, a size of 3 × 3 × 20 mm³ N_p-cut KGW was placed behind Nd:YVO₄ crystal to generate the first Stokes field as shown in Figure 1b. Two LBO crystals, with different cutting angle $\theta = 90^\circ$ and $\varphi = 3.9^\circ$; $\theta = 90^\circ$ and $\varphi = 8^\circ$, were exploited to achieve the optimal phase-matching in nonlinear process of SHG for the first Stokes field and SFG for the first Stokes field and the fundamental wave, respectively. The dimensions for both LBO crystals were 3 × 3 × 8 mm³ and the surface coatings for both were an antireflection coating at 1064 nm, 1176 nm, and 530–600 nm (reflectance < 0.2%). All laser crystals were wrapped with an indium foil and housed at an upper copper heat sink. The upper copper heat sink was mounted at the lower copper heat sink which had the water cooling at the temperature of 20 °C. For the LBO crystals, the thermoelectric cooler (TEC) was placed between the upper and lower copper heat sink. Therefore, we can precisely control the temperature of LBO crystals to obtain the optimal phase-matching. The output coupler was a concave mirror with 75 mm radius of curvature. Both facets of the output coupler were coated at high reflectance at 1050–1180 nm (R > 99%) and high transmission at 540–600 nm (T > 98%), which decreased the loss of the Stokes field and the lasing threshold. We utilized a 40 W fiber-coupled laser diode (BWT K808DNIRN-40.00W) as a pump source, which was made up of a core diameter 200 μm, a numerical aperture 0.22, and emitting central wavelength at 808 nm. The laser diode was operated at quasi-CW mode with the repetition rate 50 Hz and the duty cycle 50%. A telescope arrangement was exploited to collimate and focus the pump beam into the Nd:YVO₄ with a diameter of approximately 500 μm. The entire resonator length of self-Raman Nd:YVO₄ laser and Nd:YVO₄/KGW Raman laser were 60 mm and 65 mm, respectively.

The designed coating at the facet of KGW toward the Nd:YVO₄ was highly reflective at 1150–1180 nm (R > 98%) and highly transmissive at 1064 nm (T > 95%) as shown in Figure 2a. By applying this coating on the surface of KGW crystal, the resonators of Stokes field and that of fundamental wave were totally separated. In order to prevent the visible lights to propagate into the gain medium or Raman medium which caused the reabsorption and decreased the output powers, the highly reflective at 530–590 nm (R > 99.5%) was coated on the other facet of 20 mm Nd:YVO₄ crystal and KGW crystal as shown in Figure 2b.

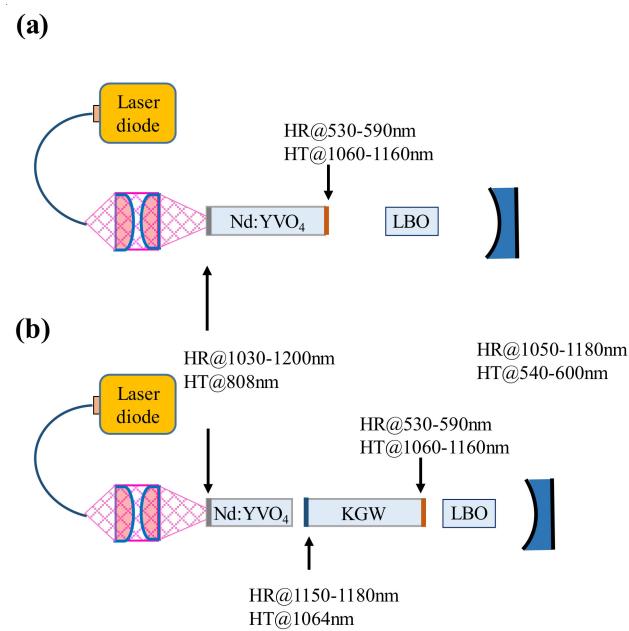


Figure 1. Experimental setup of the diode-pumped (a) self-Raman Nd:YVO₄ lasers and (b) Nd:YVO₄/KGW Raman lasers with intracavity SFG and SHG for accomplishing the lime and orange wavelengths.

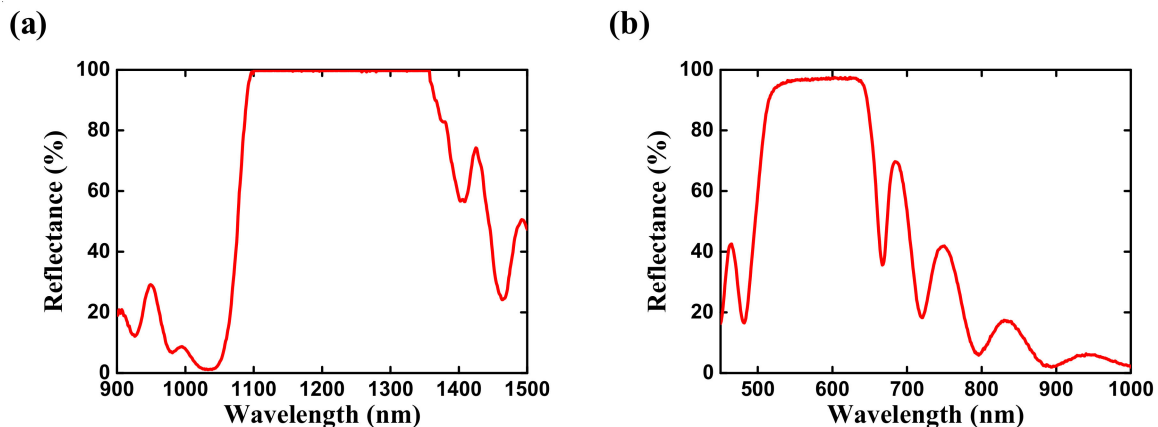


Figure 2. (a) The Reflectance spectrum of coating on the facet of KGW crystal toward the Nd:YVO₄ crystal; (b) The other facet of KGW crystal coating highly reflective at visible.

3. Results and Discussion

Figure 3a demonstrates the output power at 559 nm versus the incident pump power. The temperature of LBO crystal ($\theta = 90^\circ$ and $\varphi = 8^\circ$) was maintained at 24°C to obtain the optimal phase-matching. We measured the output power by a thermal power sensor (THORLABS S425C-L). For the self-Raman Nd:YVO₄ laser, the lasing threshold was approximately at 0.8 W and the output power was up to 6.54 W at the incident pump power of 40 W, with an optical conversion efficiency of 16.4%. In contrast to the self-Raman Nd:YVO₄ laser, the lasing threshold of Nd:YVO₄/KGW Raman laser was measured near 3 W. The higher threshold reflects that inserting KGW crystal can lead to the insertion losses of laser cavity. However, the thermal lens issue can be simply solved by sharing the numerous thermal loading by the KGW crystal. Accordingly, the output power at 559 nm can be considerably improved to 9.1 W at the incident pump power of 40 W, and an optical conversion efficiency was calculated to 22.8%. At the pump power below 30 W, it was found that the overall output power in the self-Raman Nd:YVO₄ laser was higher than that

in Nd:YVO₄/KGW Raman laser as shown in Figure 3a. On the other hand, when the pump power reached 30 W, the growth of output power started to saturation in the self-Raman Nd:YVO₄ laser, which was attributed to the strong thermal lens from the Nd:YVO₄ crystal.

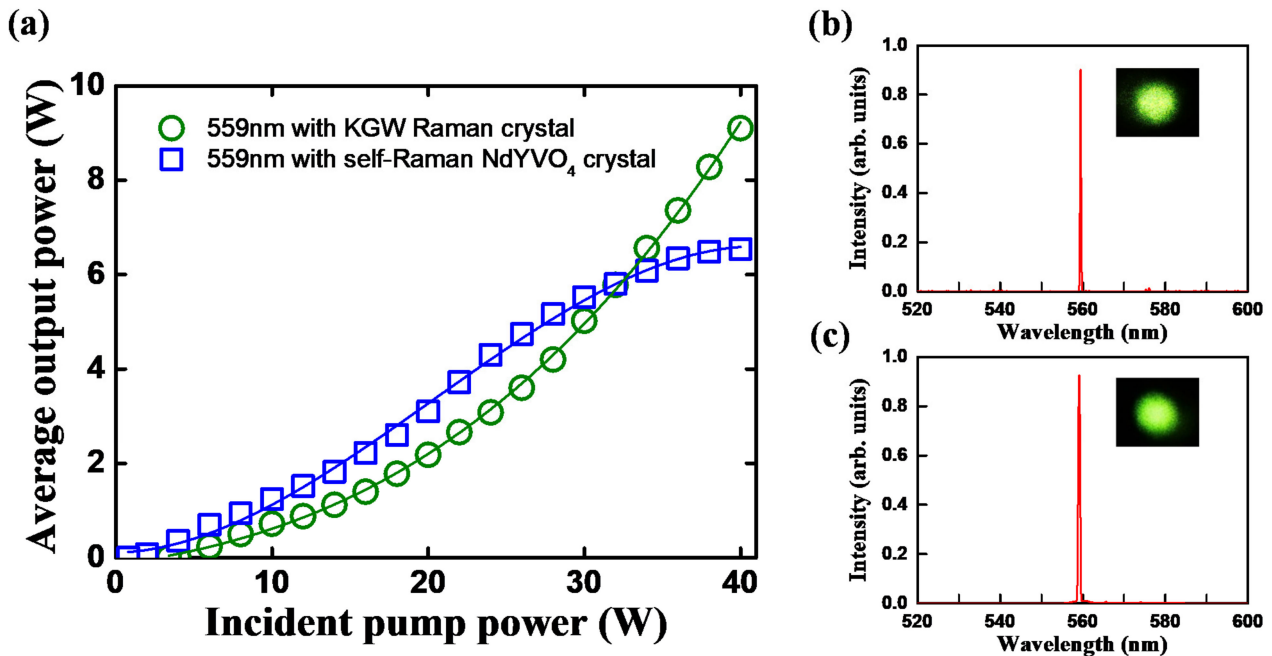


Figure 3. (a) The output power at 559 nm versus the incident pump power. Optical spectra of 559 nm wavelength and corresponding transverse mode patterns in the (b) self-Raman Nd:YVO₄ laser and (c) Nd:YVO₄/KGW Raman laser.

Besides, due to the properties of KGW crystal such as anisotropic thermal expansion coefficients and negative thermal lens, the Nd:YVO₄/KGW Raman laser is more suitable for operating at high pump power [25]. Figure 3b,c show the lasing spectrums and the transverse patterns of self-Raman Nd:YVO₄ laser and Nd:YVO₄/KGW Raman laser at the incident pump power of 10 W, respectively. The optical spectrum was monitored by an optical spectrum analyzer (Advantest Q8381A) with a resolution of 0.1 nm. The transverse pattern was imaged by a CCD camera at the distance $z \approx 8z_R$ behind the beam waist, where z_R is Rayleigh length. The M^2 factors were found to be approximately 3.0 ± 0.5 for self-Raman Nd:YVO₄ laser and Nd:YVO₄/KGW Raman laser at 559 nm by utilizing laser beam diagnostics.

In addition to the output performance of 559 nm, Figure 4a also shows the output power at 588 nm and 589 nm as the function of the incident pump power. The other LBO crystal ($\theta = 90^\circ$ and $\varphi = 3.9^\circ$) was exploited here to accomplish SHG of the first Stokes field at the temperature of 22 °C. The lasing threshold of 588 nm was equal to that of 559 nm in the self-Raman Nd:YVO₄ laser. The output power of 5.12 W at 588 nm was achieved at the incident pump power of 40 W. However, by using the Nd:YVO₄/KGW Raman laser that we mentioned above, the output power of 7.5 W at 589 nm was obtained, with the lasing threshold at 2.2 W. At the pump power below 20 W, the overall output power in the self-Raman Nd:YVO₄ laser was slightly higher than that in the Nd:YVO₄/KGW Raman laser. Nevertheless, at high pump power regions, the self-Raman Nd:YVO₄ laser also reflected the thermal loading in the saturation of output power. The corresponding optical conversion efficiency can be increased from 12.8% to 18.8%. The lasing spectrums and the transverse patterns were also shown in Figure 4b,c. The M^2 factor for both lasers at 588 nm and 589 nm was estimated to 3.0 ± 0.5 . Furthermore, the output fiber coupling efficiency of all lasers were found to be $90 \pm 2\%$ and $88 \pm 2\%$ at the pump power of 10 W and 40 W by a 50 μm multi-mode fiber with the focusing lens $f = 15$ mm.

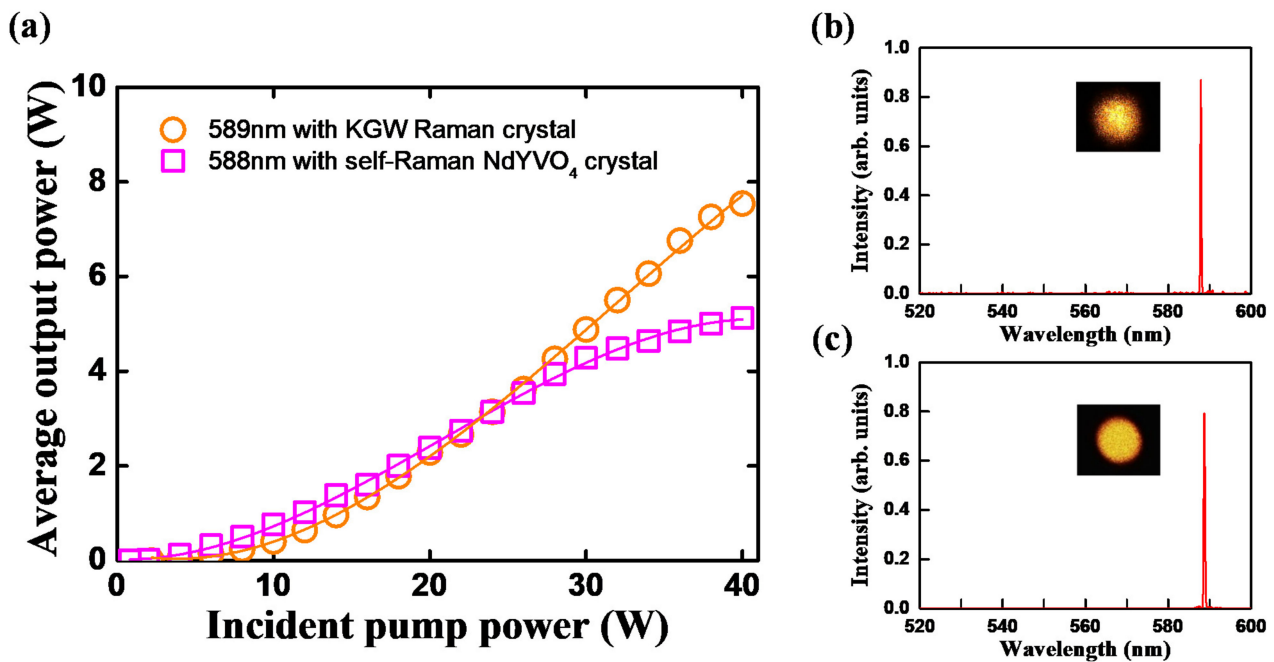


Figure 4. (a) The output power at 588 nm and 589 nm versus the incident pump power. Optical spectra of 588 nm and 589 nm wavelengths and corresponding transverse mode patterns in the (b) self-Raman Nd:YVO₄ laser and (c) Nd:YVO₄/KGW Raman laser.

It is worthwhile to mention that both laser systems have their advantages and disadvantages. For example, although the self-Raman Nd:YVO₄ lasers are not competitive to the Nd:YVO₄/KGW Raman laser at the high pump power, the lower thresholds and the short resonator are also fulfilled with some applications that do not require such high output power. Consequently, we can flexibly select the way to generate the wavelengths at lime and orange depending on the requirements of applications.

4. Conclusions

In conclusion, we have thoroughly completed the comparison between self-Raman Nd:YVO₄ lasers and Nd:YVO₄/KGW Raman lasers at lime and orange wavelengths. By using KGW crystal to accomplish the SRS process, the thermal loading can obviously decrease in the Nd:YVO₄/KGW Raman lasers than the self-Raman Nd:YVO₄ lasers, especially in the high pump power. Furthermore, employing the highly reflective coating for the first Stokes field on the facet of KGW crystal not only improved the beam quality, but also reduced the lasing thresholds. For the self-Raman Nd:YVO₄ lasers, the output powers of 6.54 W and 5.2 W at 559 nm and 588 nm have been achieved at the incident pump power of 40 W. Moreover, for the Nd:YVO₄/KGW Raman lasers, the output powers at 559 nm and 589 nm have been up to 9.1 W and 7.5 W. We believe that the high-power Nd:YVO₄/KGW Raman lasers at the 559 nm and 589 nm are available commercially for many applications.

Author Contributions: Conceptualization, C.-C.L. and C.-H.T.; validation, C.-M.C. and C.-C.L.; formal analysis, H.-Y.H. and C.-Y.H.; resources, H.-Y.H. and C.-Y.H.; writing—original draft preparation, C.-C.L.; writing—review and editing, C.-C.L., C.-M.C. and C.-H.T.; supervision, C.-H.T. All authors have read and agreed to the published version of the manuscript.

Funding: This work is supported by the Ministry of Science and Technology of Taiwan (contract number 109-2112-M-009-015-MY3).

Institutional Review Board Statement: Not applicable.

Informed Consent Statement: Not applicable.

Data Availability Statement: All of the data reported in the paper are presented in the main text. Any other data will be provided on request.

Conflicts of Interest: The authors declare no conflict of interest.

References

1. Voliani, V.; Signore, G.; Vittorio, O.; Faraci, P.; Luin, S.; Pérez-Prieto, J.; Beltram, F. Cancer phototherapy in living cells by multiphoton release of doxorubicin from gold nanospheres. *J. Mater. Chem. B* **2013**, *1*, 4225–4230. [[CrossRef](#)]
2. Palanker, D.; Blumenkranz, M.S.; Weiter, J.J. Retinal laser therapy: Biophysical basis and applications. *Protein Sci.* **2016**, *1*, 4.
3. Zhang, L.; Jiang, H.; Cui, S.; Hu, J.; Feng, Y. Versatile Raman fiber laser for sodium laser guide star. *Laser Photonics Rev.* **2014**, *8*, 889–895. [[CrossRef](#)]
4. Jansen, M.; Cantos, B.D.; Carey, G.P.; Dato, R.; Giaretta, G.; Hallstein, S.; Hitchens, W.R.; Lee, D.; Mooradian, A.; Nabiev, R.F.; et al. Visible laser and laser array sources for projection displays. *Proc. SPIE* **2006**, *6135*, 61350T.
5. Lü, Y.; Zhang, X.; Li, S.; Xia, J.; Cheng, W.; Xiong, Z. All-solid-state cw sodium D₂ resonance radiation based on intracavity frequency-doubled self-Raman laser operation in double-end diffusion-bonded Nd³⁺: LuVO₄ crystal. *Opt. Lett.* **2010**, *35*, 2964–2966. [[CrossRef](#)]
6. Chen, Y.F.; Liu, Y.C.; Gu, D.Y.; Pan, Y.Y.; Cheng, H.P.; Tsou, C.H.; Liang, H.C. High-power dual-color yellow–green solid-state self-Raman laser. *Laser Phys.* **2019**, *29*, 075802. [[CrossRef](#)]
7. Kananovich, A.; Demidovich, A.; Danailov, M.; Grabtchikov, A.; Orlovich, V. All-solid-state quasi-CW yellow laser with intracavity self-Raman conversion and sum frequency generation. *Laser Phys. Lett.* **2010**, *7*, 573–578. [[CrossRef](#)]
8. Li, X.; Pask, H.M.; Lee, A.J.; Huo, Y.; Piper, J.A.; Spence, D.J. Miniature wavelength-selectable Raman laser: New insights for optimizing performance. *Opt. Express* **2011**, *19*, 25623–25631. [[CrossRef](#)] [[PubMed](#)]
9. Dekker, P.; Pask, H.M.; Spence, D.J.; Piper, J.A. Continuous-wave, intracavity doubled, self-Raman laser operation in Nd:GdVO₄ at 586.5 nm. *Opt. Express* **2007**, *15*, 7038–7046. [[CrossRef](#)] [[PubMed](#)]
10. Lee, A.J.; Spence, D.J.; Piper, J.A.; Pask, H.M. A wavelength-versatile, continuous-wave, self-Raman solid-state laser operating in the visible. *Opt. Express* **2010**, *18*, 20013–20018. [[CrossRef](#)]
11. Tan, Y.; Fu, X.H.; Zhai, P.; Zhang, X.H. An efficient cw laser at 560 nm by intracavity sum-frequency mixing in a self-Raman Nd:LuVO₄ laser. *Laser Phys.* **2013**, *23*, 045806. [[CrossRef](#)]
12. Chen, Y.F.; Pan, Y.Y.; Liu, Y.C.; Cheng, H.P.; Tsou, C.H.; Liang, H.C. Efficient high-power continuous-wave lasers at green–lime–yellow wavelengths by using a Nd:YVO₄ self-Raman crystal. *Opt. Express* **2019**, *27*, 2029–2035. [[CrossRef](#)] [[PubMed](#)]
13. Lee, A.J.; Pask, H.M.; Piper, J.A.; Zhang, H.; Wang, J. An intracavity, frequency-doubled BaWO₄ Raman laser generating multi-watt continuous-wave, yellow emission. *Opt. Express* **2010**, *18*, 5984–5992. [[CrossRef](#)]
14. Jakutis-Neto, J.; Lin, J.; Wetter, N.U.; Pask, H. Continuous-wave watt-level Nd:YLF/KGW Raman laser operating at near-IR, yellow and lime-green wavelengths. *Opt. Express* **2012**, *20*, 9841–9850. [[CrossRef](#)] [[PubMed](#)]
15. Chen, Y.F.; Huang, H.Y.; Lee, C.C.; Hsiao, J.Q.; Tsou, C.H.; Liang, H.C. High-power diode-pumped Nd:GdVO₄/KGW Raman laser at 578 nm. *Opt. Lett.* **2020**, *45*, 5562–5565. [[CrossRef](#)]
16. Zhang, L.; Duan, Y.; Sun, Y.; Chen, Y.; Li, Z.; Zhu, H.; Zhang, G.; Tang, D. Passively Q-switched multiple visible wavelengths switchable YVO₄ Raman laser. *J. Lumin.* **2020**, *228*, 117650. [[CrossRef](#)]
17. Runcorn, T.H.; Görlitz, F.G.; Murray, R.T.; Kelleher, E.J. Visible Raman-shifted fiber lasers for biophotonic applications. *IEEE J. Sel. Top. Quantum Electron.* **2017**, *24*, 1–8. [[CrossRef](#)]
18. Xu, L.; Alam, S.; Kang, Q.; Shepherd, D.P.; Richardson, D.J. Raman-shifted wavelength-selectable pulsed fiber laser with high repetition rate and high pulse energy in the visible. *Opt. Express* **2017**, *25*, 351–356. [[CrossRef](#)]
19. Chen, Y.F.; Chen, C.M.; Lee, C.C.; Huang, H.Y.; Li, D.; Hsiao, J.Q.; Tsou, C.H.; Liang, H.C. Efficient solid-state Raman yellow laser at 579.5 nm. *Opt. Lett.* **2020**, *45*, 5612–5615. [[CrossRef](#)] [[PubMed](#)]
20. Chen, Y.F.; Li, D.; Lee, Y.M.; Lee, C.C.; Huang, H.Y.; Tsou, C.H.; Liang, H.C. Highly efficient solid-state Raman yellow–orange lasers created by enhancing the cavity reflectivity. *Opt. Lett.* **2021**, *46*, 797–800. [[CrossRef](#)]
21. Chen, Y.F. Efficient 1521-nm Nd:GdVO₄ Raman laser. *Opt. Lett.* **2004**, *29*, 2632–2634. [[CrossRef](#)]
22. Demidovich, A.A.; Grabtchikov, A.S.; Lisinetskii, V.A.; Burakevich, V.N.; Orlovich, V.A.; Kiefer, W. Continuous-wave Raman generation in a diode-pumped Nd³⁺: KGd(WO₄)₂ laser. *Opt. Lett.* **2005**, *30*, 1701–1703. [[CrossRef](#)] [[PubMed](#)]
23. Piper, J.A.; Pask, H.M. Crystalline Raman lasers. *IEEE J. Sel. Top. Quant. Electron.* **2007**, *13*, 692–704. [[CrossRef](#)]
24. Grabtchikov, A.S.; Kuzmin, A.N.; Lisinetskii, V.A.; Ryabtsev, G.I.; Orlovich, V.A.; Demidovich, A.A. Stimulated Raman scattering in Nd:KGW laser with diode pumping. *J. Alloy. Compd.* **2000**, *300*, 300–302. [[CrossRef](#)]
25. Mochalov, I.V. Laser and nonlinear properties of the potassium gadolinium tungstate laser crystal KGd(WO₄)₂:Nd³⁺-(KGW:Nd). *Opt. Eng.* **1997**, *36*, 1660–1669. [[CrossRef](#)]